Effect of crystalline domain size on the photophysical properties of thin organic molecular films

A. J. Mäkinen*
Department of Physics and Astronomy, and Center for Photoinduced Charge Transfer, University of Rochester, Rochester, New York 14627

A. R. Melnyk
Xerox Corporation, Webster, New York 14580

S. Schoemann
Center for Photoinduced Charge Transfer, University of Rochester, Rochester, New York 14627

R. L. Headrick
Cornell High Energy Synchrotron Source, Cornell University, Ithaca, New York 14853

Yongli Gao
Department of Physics and Astronomy, University of Rochester, Rochester, New York 14627
(Received 28 June 1999)

We have studied two distinct morphologies of vacuum evaporated thin N,N'-bis(phenethyl)-perylene-3,4:9,10-bis(dicarboximide) (DPEP) films with high-intensity synchrotron radiation. Layers deposited on glass or silicon dioxide substrates are shown to be highly oriented polycrystalline films with the [001] crystal axis normal to the substrate surface, and a mosaicity less than 0.02°. Transverse x-ray scans through the (002) reflection reveal diffuse scattering from that the lateral domain sizes of the films can be measured. Fast evaporation of DPEP onto cooled substrates results in a bright red film that is found to have a grain structure with a domain size of 250 Å. Slower evaporation onto heated substrate produces a film of green color with a more than one order of magnitude larger domain size of 3300 Å. The domain sizes and shapes extracted from the x-ray data agree well with separately recorded atomic force microscopy images of the DPEP films. The obtained crystal structure and submicron domain size of the large-grain DPEP film explain the recently reported extremely long exciton transfer lengths in polycrystalline DPEP films.
[S0163-1829(99)00145-9]

I. INTRODUCTION

The absorption spectrum of an organic solid is largely determined by the interplay between the absorption properties of a single molecule and the local environment of the molecule in the solid. The absorption process subsequently leads to the formation of a variety of different collective excited states, such as Frenckel excitons and charge-transfer excitons,[1,2] which are ultimately responsible for phenomena such as photocharge generation and charge transfer in organic molecular thin films. However, these steady-state excitons are delocalized within the entire crystal.[3] Therefore, the properties of excitons depend upon the structure of the crystal as a whole. A full understanding of the photophysics of an organic semiconductor requires a detailed knowledge of the crystalline structure of the material. This includes information about the crystalline phase, as well as the domain size and the distribution of crystallite orientations.

N,N'-bis(phenethyl)-perylene-3,4:9,10-bis(dicarboximide) (DPEP) is known to form a number of different polymorphs.[4] They can be produced by varying film evaporation conditions in order to produce different phases,[5] or by solvent treatment of an evaporated film in order to induce crystallization.[6,7] Both the absorption spectrum and the photocharge generation efficiency of DPEP films have been shown to depend on the crystalline phase of the films.[8,9] Recently, a singlet exciton-transfer length of 2.5 μm has been reported for a polycrystalline DPEP film.[10] This long exciton-transfer length indicates that a significant degree of delocalization of the excitons in the molecular lattice can occur.

In this paper, we report the results of a high-resolution synchrotron x-ray diffraction study of thin DPEP films. We have studied films with two distinct microstructures, prepared through vacuum evaporation without solvent treatment. These films are identified primarily through their starkly different absorption spectra, which give them a characteristic color. The first type, which we call DPEP-I is bright red in color. It is produced by fast deposition of the molecules onto cooled substrates. The second type, which we call DPEP-II, has a green color, and is produced by slow deposition of the molecules onto heated substrates. The x-ray diffraction results suggests that DPEP-I is predominantly composed of amorphous material, although small grains of crystalline material are present. DPEP-II exhibits a strikingly different structure. It can be described as a large-domain polycrystalline material, highly oriented along the surface normal of the film. These results suggest that the difference in the absorption spectra between the two types of films is a result of a different molecular packing in amorphous and

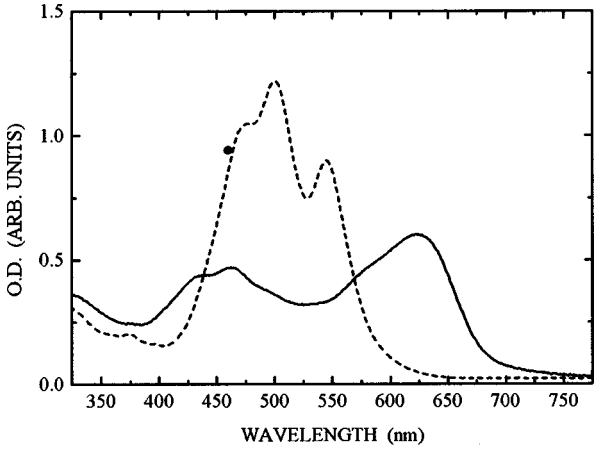

FIG. 1. Absorption spectra of DPEP-I film (dashed line) evaporated onto a cooled glass substrate at $-60\,^{\circ}\mathrm{C}$ with an evaporation rate of 8 Å/s and DPEP-II film (solid line) evaporated onto a heated glass substrate at 110°C with an evaporation rate of 1 Å /s. Both films were 2500 Å thick.

crystalline materials. The large well-oriented domains of DPEP-II are consistent with an interpretation where strong exciton-exciton coupling results in delocalization of the exciton within a single crystallite. This explains the extremely long-range charge and energy-transfer processes observed by Gregg *et al.*[10] The highly orientated crystallites in the films are expected to further reduce scattering of excitons at grain boundaries for charge and energy transfer along the surface normal.

II. EXPERIMENT

The samples were made by vacuum evaporating (base pressure 1×10^{-9} torr) DPEP from a resistively heated Ta source boat onto thermally oxidized Si(100) or indium tin oxide (ITO)-covered glass substrates. The morphology of the film was controlled by varying the substrate temperature and the deposition rate. For the experiments described in this paper, we generated two film structures characterized by very different absorption spectra and film colors. The film with an absorption maximum at 500 nm (DPEP-I) was evaporated at the substrate temperature of $-60\,^{\circ}\mathrm{C}$ and with an evaporation rate of 8 Å /s. The film with absorption maximum at 630 nm (DPEP-II) was evaporated at an elevated substrate temperature of $110\,^{\circ}\mathrm{C}$ with an evaporation rate of 1 Å /s.

The absorption spectra (UV Spectrophotometer; Perkin Elmer) of the two films evaporated on glass substrates are shown in Fig. 1. It is clear from the figure that the film morphology has a pronounced effect on the absorption properties of DPEP films. The absorption spectrum of DPEP-I shows the vibrational levels of S_1 states that are both broadened and redshifted compared with the solution spectrum of DPEP.[7] The broadening and the shift of the spectral peaks are attributed to the polarization effects present in the solid state.[11] The polymorph of the DPEP-I film has previously been described in the literature as an amorphous phase[6,5] where molecules are more or less randomly oriented. We, however, have a reason to suggest that the composition of the DPEP-I film is small crystalline grains embedded in

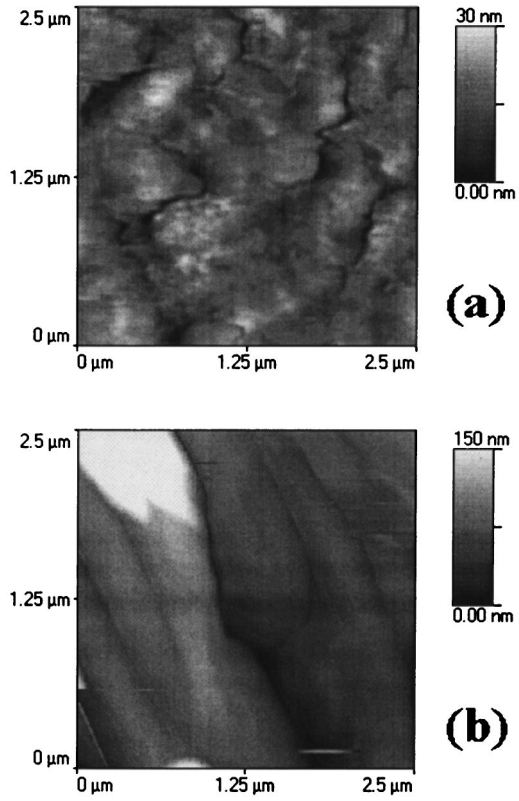

FIG. 2. AFM scans of (a) DPEP-I and (b) DPEP-II films.

amorphous material, which will become evident from the discussion of the x-ray-diffraction (XRD) results later in this paper. The absorption spectrum of DPEP-II shows a further broadened S_1 band whose long wavelength part is redshifted. The spectrum compares well with similar spectra of solvent-treated DPEP films,[8] and polycrystalline films created directly through vacuum evaporation[5] reported in the literature. The extended states forming in the long wavelength region are attributed to intermolecular interactions found in more ordered DPEP-II films,[7] which is also used to explain the greater photocharge generation efficiency of these films.[9]

Atomic force microscopy (AFM) was performed on the evaporated DPEP films in air using the Topometrix Explorer. The effect of different evaporation conditions can clearly be seen in the AFM images in Fig. 2. The AFM image of the DPEP-I film shows no regular pattern but randomly distributed valleys and hills. The root-mean-square roughness (RMSR) is relatively low, $\sim$8 nm. Conversely, the AFM image of the DPEP-II film shows large needlelike crystallites with domain sizes up to 150 nm $\times$500 nm$\times$2500 nm. The corresponding RMSR is much higher in this case, $\sim$35 nm.

The x-ray-diffraction experiment was carried out at the F3 station of Cornell High Energy Synchrotron Source (CHESS). The sample was mounted at the center of a standard four-circle diffractometer. The incident x-ray energy and flux were 10.2 keV and 3×10^{11} photons/s, respectively, provided by a pair of Si(111) monochromator crystals. The instrument resolution was determined at the (002) Bragg position, and was found to be 1.4×10^{-4} Å^{-1} in the q_x, 8.2×10^{-2} Å^{-1} in the q_y, and 2.0×10^{-1} Å^{-1} in the q_z direction. The detector was a NaI scintilator.

Both DPEP-I and DPEP-II films evaporated on thermally

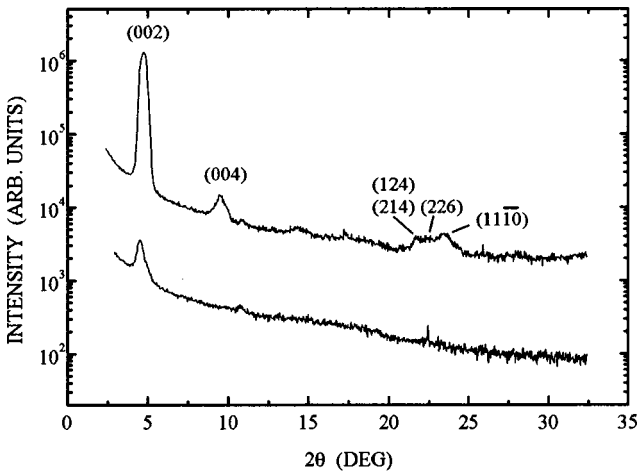

FIG. 3. XRD spectra of DPEP-I (bottom curve) and DPEP-II films (top curve). The labels indicate the crystal directions of the Bragg reflections in the DPEP-II film.

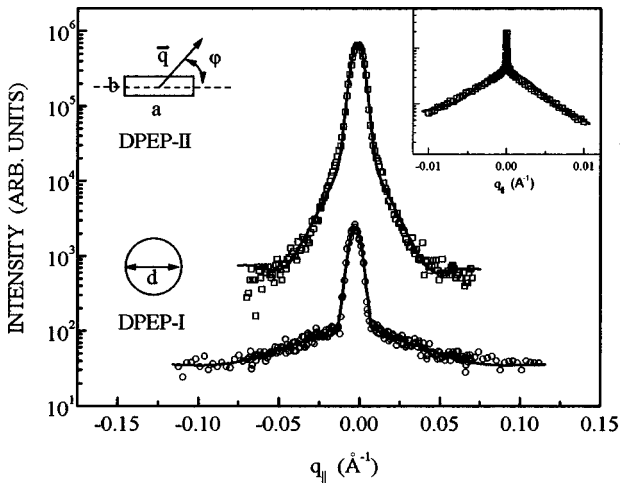

FIG. 4. Diffuse scattering intensities for DPEP-I (circles) and DPEP-II (squares) films with fits to the line shapes (solid lines) given in the text. The insets on the left show the two geometries for calculating the line shapes. The inset on the right shows a high-resolution transverse scan of the DPEP-II film. The best fit values for the parameters are $a=3300$ Å, $b=390$ Å, $d=250$ Å. The FWHM of the specular part is 0.0082 Å^{-1} in the two lower-resolution scans and 1.4×10^{-4} Å^{-1} in the high-resolution scan.

oxidized Si(111) substrates have very clear first-order Bragg reflections in the (002) direction as seen in their diffraction spectra shown in Fig. 3. Since this Bragg reflection indicates a momentum transfer normal to the surface, this implies that although the AFM images show a rather disordered surface topology for the DPEP-I film, there is a significant amount of order in the vertical crystal direction of the film. The DPEP-II film shows additional Bragg reflections at higher angle values that are absent in the DPEP-I spectrum. Further, the first-order peak of DPEP-I at $2\theta=4.52°$ is shifted down from the corresponding peak of DPEP-II at $2\theta=4.77°$.

III. ANALYSIS

The assignment of Bragg peaks of the DPEP-II film to different lattice directions was done by computing the structure factor of the known DPEP crystal structure[12–14] and by comparing the calculated peak positions with the observed ones. The (002) and (004) reflections are within 0.02° of the calculated 2θ values, and the (214), (226), and (11-10) directions fall within 0.06° of the calculated values. It is important to note that all the observed Bragg reflections are more or less in [001] direction, which is an indication of a highly oriented film. The first- and second-order peaks are, however, relatively broad, FWHM $\sim0.2°$, which is attributed to a distribution of lattice parameter values. The DPEP films evaporated onto ITO-covered glass substrates showed the same Bragg peak positions as the films on thermally oxidized Si substrates, and therefore this allows us to exclude any substrate-induced effects in the data.

Diffuse scattering intensities shown in Fig. 4 were measured by transverse scans near the first-order (002) Bragg reflection of the DPEP-I and the DPEP-II films. Apart from the total intensities, the line shapes of the two spectra seem to have similar general features. Both the spectra have a narrow central specular part and broader diffuse part that makes up the wing regions of the spectrum. The width of the specular part is instrument limited and it originates from the vertical order present in the films as mentioned earlier. The important distinction between the spectra of the two films is the much broader diffuse scattering part of the DPEP-I film.

The line shape of the transverse scan intensity can be treated as a superposition of the specular I_S and diffuse I_D components, i.e.,

$$I=I_S+I_D, \tag{1}$$

where the specular component is described as a narrow Gaussian function, $I_S(q)=A\exp(-q^2/2\sigma^2)$. The diffuse scattering intensities of x-rays near Bragg peaks are known to contain information about the short-range correlation and the structural order in a crystal lattice. In this case, the line shape for the diffuse scattering is determined by the finite-size of the crystal domains in the lateral direction of the DPEP films. If the finite-size sources are assumed to be mostly uncorrelated in the lateral directions the line shape can be expressed as a convolution of the structure factor and the shape function of a single-crystal domain.[15] Based on the needle-shaped crystal domains revealed by the AFM image of the DPEP-II film surface, we have approximated the crystal shape in the DPEP-II film with a rectangle of dimensions $a\times b$. We have further assumed the lateral direction of the crystal domain orientation (angle φ in the inset of Fig. 4) to be random. The line shape of the diffuse scattering intensity now becomes

$$I_D(q)=a^2b^2\int_{-\pi/2}^{\pi/2}d\varphi\frac{\sin^2(\pi aq\sin\varphi)}{(\pi aq\sin\varphi)^2}\frac{\cos^2(\pi bq\sin\varphi)}{(\pi bq\cos\varphi)^2}, \tag{2}$$

where the integration is done numerically. For the DPEP-I films, a different kind of geometry needs to be considered. The AFM image of the DPEP-I film shows no regular crystal shape, and hence we have chosen to treat the DPEP-I domains as circular disks. The diffuse scattering is given in this case by

$$I_D(q) = d^2\left[\frac{J_1(\pi dq)}{\pi dq}\right]^2, \quad (3)$$

where d is the diameter of the disk and J_1 is the first-order Bessel function.

Apart from the amplitudes, the only parameters included in the expressions (2) and (3) are the dimensions of the crystals, i.e., parameters a, b, and d. This provides a relatively simple model for analyzing the diffuse scattering in the DPEP films. Fitting the line-shape functions to the transverse scan data (see Fig. 4) gives the best-fit values of 3300 Å and 390 Å for the DPEP-II domain dimensions a and b, respectively, and 250 Å for the DPEP-I domain dimension d. The full width at half maximum (FWHM) of the specular part is 0.0082 $Å^{-1}$ in both cases. The inset in Fig. 4 shows a high-resolution transverse scan of the DPEP-II film. The line-shape fit is the same as for the lower-resolution scan of the DPEP-II film except the FWHM of the specular part, which in this case is 1.4×10^{-4} $Å^{-4}$. The extremely narrow specular part in the high-resolution scan indicates a low mosaicity of the DPEP films (less than 0.02°), and therefore eliminates the possible contribution from the film mosaicity to the diffuse parts of the transverse scans.

IV. DISCUSSION

The line-shape functions seem to describe the data well given the simplicity of the model. The observed deviations between the fits and the data are attributed to the fact that in the model, essentially a single-crystal domain size has been used to replace a distribution of domain sizes found in the films. In fact, the expressions (2) and (3) could be convolved with the size distribution of crystals in the film, and the resulting functions would probably better describe the diffuse part of the scattering. Since neither the exact size distribution is known nor a reasonable estimate for it is available we will treat the value of the crystal domain dimension found from the fit as the typical size of the crystal domain in the film. The deduced lateral domain size, 390 Å $\times$ 3300 Å, for the DPEP-II film compares reasonably well with the domains observed in the AFM image of the film in Fig. 2(b), therefore supporting the results of the line-shape analysis.

The clearest distinctions between the DPEP-I and the DPEP-II films are the different absorption spectra of the films and the lateral domain sizes the latter of which are now confirmed by both the diffuse scattering of the x rays in the films and the AFM images of the film surfaces. An interesting question is whether the domain sizes are in any way related to the absorption properties, i.e., whether there are any size-induced effects. Detailed fluorescence studies on quantum-well structures of 3,4,9,10-perylenetetracarboxylic dianhydride (PTCDA) and 3,4,7,8-naphtalenetetracarboxylic dianhydride (NTCDA), which both have an analogous molecular and crystal structure to DPEP, have shown that the quantum confinement effects are considerable only for well widths less than 100 Å.[16,17] The model calculations combined with electroabsorption results on PTCDA films have determined the charge-transfer (CT) exciton radius to be 10–12 Å long.[1] The DPEP-I domain size, 250 Å in diameter, is more than twice the limit for the quantum confinement observed for PTCDA and therefore we do not expect the smaller domain size in DPEP-I films to influence the absorption properties.

The most obvious explanation for the different absorption properties of the DPEP-I and the DPEP-II films is that the former is an amorphous film and the latter is a crystalline film. As mentioned earlier, the amorphousness of the DPEP-I film is also suggested by the close resemblance between its absorption spectrum and the solution spectrum of the DPEP molecule. However, if we assume DPEP-I to be mostly amorphous we will have to explain the observed first-order Bragg reflection of the DPEP-I film. The two orders of magnitude difference in the first-order peak intensities of the DPEP-I and the DPEP-II Bragg reflection data (see Fig. 4) seems to offer an explanation. If we take the ratio of the integrated area under the peaks, we get an approximation for the square of the ratio of the amounts of crystalline material in the DPEP-I and the DPEP-II films. This ratio is ~0.02, i.e., the amount of crystalline material in the DPEP-I film is about 14% of the corresponding amount in the DPEP-II film. In other words, the composition of the DPEP-I film is most likely to be a mixture of small crystalline grains and amorphous material. Therefore, DPEP molecules show a considerable degree of aggregation even in the least favorable growth conditions (fast evaporation onto cooled substrates). This indicates the presence of a strong chemical potential driving the aggregation process. In general, large semirigid molecules have a tendency to form crystals, in which the molecules are often arranged in stacked pairs.[18]

We also want to note that the possibility of birefringence-induced contributions in the absorption spectrum of the DPEP-I film is eliminated by the following two observations. First, The Bragg reflections in DPEP-I are absent in the other two crystal directions, [100] and [010]. In other words, if the absorption spectrum of DPEP-I had contributions from the absorption along the a and b axis of crystallites we would expect to see the corresponding Bragg reflections. However, this is not the case. Second, the absorption spectrum of a dispersion of DPEP microcrystals in polystryrene is practically identical to the absorption spectrum of DPEP-II.[12] Since the absorption spectrum of this molecular dispersion is in essence the spacial average of the various absorption axis of a DPEP crystal, this observation, in fact, eliminates the possibility that the absorption spectrum of DPEP-I could be a superposition of absorptions along different crystal axis.

Model calculations have shown that a strong coupling found between molecular excitons in the DPEP-II film is responsible for the spectral displacement and the splitting of the absorption band compared with the disordered phase of DPEP.[7] The calculated values for the shifts agree reasonably well with the experimental ones, and it is found that most of the contribution to the redshift comes from the stacked pairs of molecules. Interestingly, these calculations are based on a dipole-dipole approximation for the coupling, where only the interaction between the nearest neighbors needs to be considered. This implies that the absorption properties of the DPEP films are really determined by the relatively short-range order in the molecular lattice. The significance of short-range interactions is a general property of molecular crystals, and similar effects of exciton coupling have been shown for naphtalene, anthrace, pentacene, and pure perylene crystals.[19]

A strong exciton coupling in the DPEP-II film will also influence the charge- and energy-transfer properties of the molecular film. Namely, the rate of energy transfer in molecular solids is proportional to the matrix element of dipole coupling between the excitons.[3] This combined with the large single-crystal domains of DPEP-II found in our experiments explain the recently reported long-range energy-transfer processes with length scales up to a few microns (2.5 μm) in polycrystalline DPEP films.[10] In these recent studies, it has also been suggested that the energy-transfer (exciton-transfer) process may be enhanced by the delocalization of the exciton wave function within a single crystallite. If we use the CT exciton radius found for PTCDA (10–12 Å) in the studies mentioned earlier as an estimate for the size of an exciton in DPEP-II, we find that the exciton extends over three molecular sites in DPEP-II, where the distance between the stacked pairs is $\sim$4.7 Å. In the presence of large crystal domains, such an excitation will transfer through a single-crystal domain encountering fewer grain boundaries and therefore a lower number of trap sites, which ensures the highly efficient transfer of the excitation.

V. CONCLUSION

The x-ray-diffraction study on two polymorphs of thin DPEP films shows that the films generated through vacuum evaporation are highly oriented polycrystalline films with [001] axis normal to the surface. The domain size for the coarse-grain DPEP-II film obtained from the line-shape analysis of diffuse scattering is an order of magnitude larger than the one found in the small-grain DPEP-I film, which is found to agree well with the AFM images of the DPEP film surfaces. The obtained crystal structure and submicron domain size of the DPEP-II film explain the previously observed extremely long exciton-transfer length in polycrystalline DPEP films.

ACKNOWLEDGMENTS

The authors gratefully acknowledge the National Science Foundation for Science and Technology Center Grant (No. CHE-9120001), and AFOSR for a separate grant (No. 96NL245) for the AFM work. A.J.M. acknowledges support from the Väisälä Foundation of the Finnish Science Academy.

*Electronic address: ajm@pas.rochester.edu

[1] Z. Shen and S.R. Forrest, Phys. Rev. B **55**, 10 578 (1997).
[2] M. Umeda and M. Yokoyama, J. Appl. Phys. **81**, 6179 (1997).
[3] A.S. Davydov, *Theory of Molecular Excitons* (Plenum Press, New York, 1971).
[4] P.M. Borsenberger, M.T. Regan, and W.J. Staudenmayer, U.S. Patent No. 4,578,334 (26 March 1986); U.S. Patent No. 4,618,560 (21 October 1986).
[5] M.K. Debe, K.K. Kam, J.C Liu, and R.J. Poirier, J. Vac. Sci. Technol. A **6**, 1907 (1988).
[6] B.A. Gregg, Appl. Phys. Lett. **67**, 1271 (1995).
[7] J. Mizuguchi, J. Appl. Phys. **84**, 4479 (1998).
[8] B.A. Gregg, J. Phys. Chem. **100**, 852 (1996).
[9] E.H. Magin and P.M. Borsenberger, in *Proceedings IS&T 8th International Congress in Non-Impact Printing Technologies* (IS&T, 1992), p. 243.
[10] B.A. Gregg, J. Sprague, and M.W. Peterson, J. Phys. Chem. B **101**, 5362 (1997).
[11] E.A. Silinsh, *Organic Molecular Crystals* (Springer-Verlag, Berlin, 1980).
[12] F. Graser and E. Hädicke, Liebigs Ann. Chem. **1980**, 1994; **1984**, 483.
[13] E. Hädicke and F. Graser, Acta Crystallogr., Sect. C: Cryst. Struct. Commun. **42**, 189 (1986); **42**, 195 (1986).
[14] G. Klebe, F. Graser, E. Hädicke, and J. Berndt, Acta Crystallogr., Sect. B: Struct. Sci. **B45**, 69 (1989).
[15] J.M. Cowley, *Diffraction Physics* (Elsevier, New York, 1995).
[16] F.F. So and S.R. Forrest, Phys. Rev. Lett. **66**, 2649 (1991).
[17] E.I. Haskal, Z. Shen, P.E. Burrows, and S.R. Forrest, Phys. Rev. B **51**, 4449 (1995).
[18] J. Perlstein, J. Am. Chem. Soc. **116**, 11 420 (1994).
[19] D.P. Craig and S.H. Walmsley, *Excitons in Molecular Crystals* (Benjamin, New York, 1968).